Supporting Information

Intermolecular H-bond promoting diphenylsulfone derivatives for aggregation induced blue-shifted thermally activated delayed fluorescence

Yuanping Han[a], Hanrong Liu[a], Yan Xia[b], Jie Li[b], Junhui Jia[a,*]

a. Key Laboratory of Magnetic Molecules and Magnetic Information Material of Ministry of Education, School of Chemistry and Chemical Engineering, Shanxi Normal University, Taiyuan, 030032, China

E-mail:jiajunhui@sxnu.edu.cn

b. Key Laboratory of Interface Science and Engineering in Advanced Materials, Ministry of Education, Taiyuan University of Technology, Taiyuan, 030024, China

Table of contents

1. Experimental

1.1 General Information

Unless otherwise specified, all starting chemicals and reagents were purchased from commercial sources and used as received without further purification. Solvents for synthesis were purified according to the standard procedures prior to use. NMR spectra were recorded on a Bruker NMR 600 spectrometer. Mass spectrometric measurements were performed on a ultraflex MALDI-TOF/TOF mass spectrometer, with α-cyano-4-hydroxycinnamic acid (CHCA) as the matrix. Elemental analysis was run on a Vario EL III Elemental Analyzer. UV-vis absorption spectra were recorded on a HITACHI U-3900 Spectrometer. Photoluminescence (PL) spectra were recorded on an Edinburgh Instrument FLS980 spectrometer equipped with a xenon lamp. The absolute fluorescence quantum yield of the solid was measured on an Edinburgh Instrument FLS980 spectrometer using an integrating sphere. The transient photoluminescence decay profiles were recorded using an Edinburgh Instrument FLS980 spectrometer equipped with an EPL-375 picosecond pulsed diode laser or a microseconds lamp. Thermogravimetric analysis (TGA) of the compound was conducted on a NETZSCH thermogravimetric analyzer STA 449 F5 at a heating rate of 10 °C min^{-1} under nitrogen atmosphere. Differential scanning calorimetry (DSC) measurement was carried out on a NETZSCH DSC204 instrument at a heating rate of 10 °C min^{-1} under nitrogen atmosphere. Cyclic voltammogram measurement was performed on an Autolab/PG STAT302 electrochemical analyzer at a scan rate of 50 mV/s in deoxygenated toluene solution (10^{-3} M), with 0.1 M tetra n-butylammonium hexafluorophosphate (Bu_4NPF_6) as the electrolyte and ferrocene as the internal standard. A glassy carbon working electrode, a saturated calomel electrode as the reference electrode, and a platinum wire counter electrode were used. Single-crystal X-ray diffraction data was collected on an Agilent SuperNova (Dual, Cu at zero, Eos) diffractometer. The structure was solved with the SHELXS structure solution program using direct methods and refined with the SHELXL refinement package using Least Squares minimization.

1.2 Theoretical Calculation

All density functional theory (DFT) calculations were performed using the Gaussian 09 program package. The HOMO and LUMO distribution of the compound were calculated using the B3LYP mode with 6-31g(d) basis sets. The S_n and T_n energies of the monomer and dimer were estimated by the time-dependent density functional theory (TD-DFT) method at the optimized ground-state

geometries directly selected from the single crystal structure using B3LYP at the 6-311+g(d, p) level. The SOC values were energetically optimized by density functional theory (DFT) using the Def2SVP basis set using ORCRA program. The HOMO and LUMO of the molecule, and the packing coefficient analysis of the single crystal were performed using Mulitiwfn 3.8 software package and VMD 1.9.3.

1.3 OLED device fabrication and characterization

All the OLEDs were fabricated on indium tin oxide (ITO) coated glass substrates with a sheet resistance of 10 Ω/sq. The ITO substrates were cleaned with acetone, deionized water and acetone sequentially, then treated by ultraviolet-ozone for 15 min, and then loaded into high vacuum chamber (approximately 4 × 10^{-4} Pa) for subsequent deposition. The organic layers and inorganic layers (MoO_3 and LiF) were deposited at a rate of 1.0 and 0.1 Å/s, respectively. Al cathode was deposited in the end at a rate of 5.0 Å/s with a shadow mask, which defined the device area of 3 × 3 mm^2. The voltage-current-luminance characteristics, the EL spectra and CIE coordinates were measured with PR-655 Spectra Scan Spectroradiometer and Keithley 2400 source meter unit under ambient atmosphere at room temperature. External quantum efficiencies were calculated by assuming that the devices were Lambertian light sources. The characterization of the EL performance was performed after the device was completed without encapsulation.

2. Synthesis

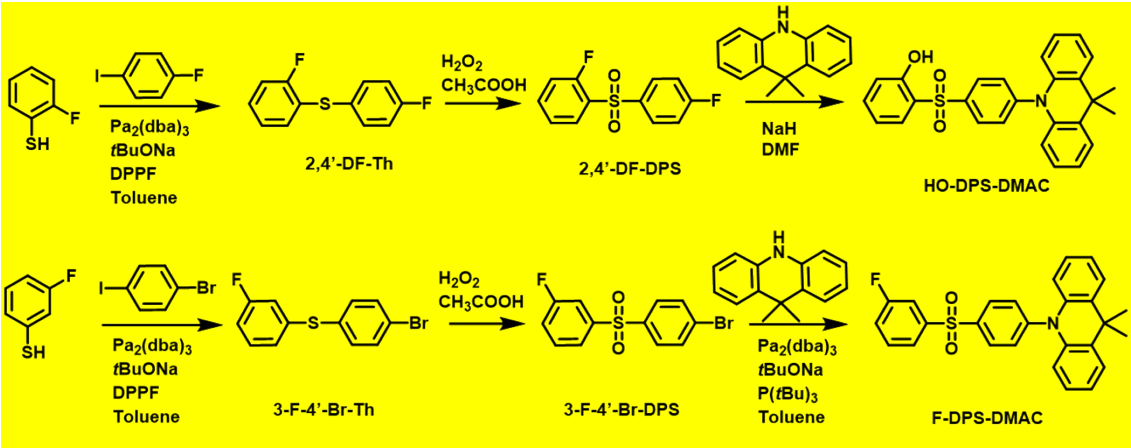

Scheme S1. Synthesis rote of compounds **HO-DPS-DMAC** and **F-DPS-DMAC**

2.1 Synthesis of bis(2,9-fluorophenyl)thioether (2,4'-DF-Th)

A mixture of 1-fluoro-2-iodobenzene (1.90 g, 8.58 mmol), 2-fluorothiophenol (1.00 g, 7.80 mmol), tris(dibenzylideneacetone)dipalladium ($Pd_2(dba)_3$, 0.18 g, 0.20 mmol), 1,1'-

bis(diphenylphosphino)ferrocene (DPPF, 0.44 mg, 0.78 mmol), sodium *tert*-butoxide (3.03 g, 78 mmol) was dissolved in toluene (30 mL) and stirred at 115 °C for 2 h. After cooling to room temperature, the reaction mixture was washed with brine for three times, dried over $MgSO_4$, and filtered. After removing the solvent under reduced pressure, the crude product was purified by column chromatography (eluent: hexane) to afford **2,4'-DF-Th** as colorless oil (1.20 g, 5.40 mmol, 75% yield). As the product was unstable, it was used for the next reaction after separation.

2.2 Synthesis of bis(2,9-fluorophenyl)sulfone (2,4'-DF-DPS)

A mixture of **2,4'-DF-Th** (1.0 g, 4.5 mmol), hydrogen peroxide solution (30%, 15 mL) and acetic acid (85%, 15 mL) was stirred at 100 °C for 5 h. After cooling to room temperature, the reaction mixture was poured into water and then filtered. The residue was washed with deionized water for three times, filtered, and then purified by column chromatography (eluent: hexane/ethyl acetate =4/1 v/v) to afford **2,4'-DF-DPS** as white solid (0.80 g, 3.10 mmol, 69%).^{1}H NMR (600 MHz，$CDCl_3$) δ 8.11-8.08 (m, 1H), 8.05-8.02 (m, 2H), 7.61-7.58 (m, 1H), 7.33 (td, J = 7.8, 1.2 Hz, 1H), 7.22-7.19 (m, 2H), 7.14-7.10 (m, 1H).

2.3 Synthesis of 2- hydroxyl-9-(9,9'-dimethyl-9, 10-dihydroacridine) phenyl sulfone (HO-DPS-DMAC)

Under nitrogen atmosphere, **2,4'-DF-DPS** (1.0 g, 3.93 mmol) and NaH (943 mg, 39.3 mmol) were added in N, N-dimethylformamid (DMF, 25 mL) and stirred at 60 °C for 0.5 h. Then 9,9-dimethyl-9,10-dihydroacridine (905 mg, 4.33 mmol) was added in the mixture and stirred at 145 °C for 12 h. After cooling to room temperature, the reaction mixture was treated with brine and then extracted with CH_2Cl_2 for three times. The combined organic solution was dried over $MgSO_4$, filtered and the solvent was removed under reduced pressure. Compound **HO-DPS-DMAC** was obtained by column chromatography (eluent: hexane/ethyl acetate = 4/1 v/v) as white solid (780 mg, 1.76 mmol). ^{1}H NMR (600 MHz, Chloroform-d) δ 9.23 (s, 1H), 8.13 (m, 2H), 7.77 (m, 1H), 7.49 (m, 5H), 7.06 (m, 2H), 6.99 (m, 4H), 6.31 (m, 2H), 1.65 (s, 6H). ^{13}C NMR (101 MHz, Chloroform-d) δ 156.09, 147.15, 140.17, 139.97, 136.47, 132.16, 130.26, 129.53, 129.38, 128.80, 126.46, 125.38, 123.33, 121.92, 121.05, 119.39, 115.42, 111.13, 40.07, 36.29, 30.64. MS (MALDI-TOF) *m/z*: $[M]^+$ calcd for 441.55, found 441.35. Anal. Calcd for $C_{27}H_{23}NO_2S$: C 73.45; H 5.25; N 3.17; found: C 73.34, H 5.47, N 3.18.

2.4 Synthesis of 3-fluorophenyl-4'-bromine thioether (3-F-4'-Br-Th)

Following the synthetic method of **2,4'-DF-Th** using 4-bromothiophenol (1.0 g, 5.29 mmol) as the

reactant (1.20 g, 4.23 mmol, 79%), **3,4'-DF-Th** was obtained as colorless oil. As the product was unstable, it was used for the next reaction after separation.

2.5 Synthesis of 3-fluorophenyl-4'-bromine sulfone (3-F-4'-Br-DPS)

Compound **3-F-4'-Br-DPS** was obtained as white solid following the synthetic method of **2,4'-DF-DPS** using **3-F-4'-Br-Th** (1 g, 3.52 mmol) as reactant (0.78 g, 2.46 mmol). ^{1}H NMR (600 MHz, $CDCl_3$) δ 7.43 (dd, J = 8.9, 1.8 Hz, 2H), 7.22 – 7.18 (m, 1H), 7.07 – 7.03 (m, 2H), 6.96 (dd, J = 7.1, 1.8 Hz, 1H), 6.87 – 6.82 (m, 2H).

2.6 Synthesis of 3- fluorophenyl-9-(9,9'-dimethyl-9, 10-dihydroacridine) phenyl sulfone (F-DPS-DMAC)

A mixture of **3-F-4'-Br-DPS** (1.0 g, 3.17 mmol), 9,9-dimethyl-9,10-dihydroacridine (729.4 mg, 3.49 mmol), $Pd_2(dba)_3$ (145 mg, 0.16 mmol), tri-*tert*-butylphosphinetetrafluoroborate (45 mg, 0.16 mmol), sodium *tert*-butoxide (3.10 g, 31.70 mmol) in toluene (15 mL) was stirred at 115 °C for 12 h. After cooling to room temperature, the reaction mixture was treated with brine and then extracted with CH_2Cl_2 for three times. The combined organic solution was dried over $MgSO_4$, filtered and removed. Compound **F-DPS-DMAC** was obtained by column chromatography (eluent: hexane/ethyl acetate = 4/1 v/v) as white solid (703 mg, 1.58 mmol). ^{1}H NMR (600 MHz, $CDCl_3$) δ 8.16 – 8.13 (m, 2H), 7.85 (td, J = 7.8, 1.7 Hz, 1H), 7.77 – 7.72 (m, 1H), 7.58 (td, J = 8.1, 5.2 Hz, 1H), 7.53 – 7.50 (m, 2H), 7.48 – 7.44 (m, 2H), 7.34 (td, J = 8.3, 1.8 Hz, 1H), 7.02 – 6.97 (m, 4H)，6.30 – 6.26 (m, 2H), 1.65 (s, 6H). ^{13}C NMR (151 MHz，$CDCl_3$) δ 163.84, 161.33, 146.92, 143.45, 140.15, 139.48, 131.93, 131.31, 130.50, 126.41, 125.36, 123.69, 121.81, 120.88, 120.67, 115.19, 36.23, 30.67. MS (MALDI-TOF) *m/z*: $[M]^+$ calcd for 444.14, found 444.14.

3. Photophysical properties of the compounds

The corresponding equations for estimating the photophysical data were as follows, [S1-S3]

$\Phi_p = \Phi_F R_p$ (eq.S1)

$\Phi_{TADF} = \Phi_F R_{TADF}$ (eq.S2)

$k_F = \Phi_p/\tau_p$ (eq.S3)

$\Phi_F = k_F/(k_F + k_{IC})$ (eq.S4)

$\Phi_p = k_F/(k_F + k_{IC} + k_{ISC})$ (eq.S5)

$\Phi_{IC} = k_{IC}/(k_F + k_{IC} + k_{ISC})$ (eq.S6)

$\Phi_{ISC} = k_{ISC}/(k_F + k_{IC} + k_{ISC}) = 1 - \Phi_p - \Phi_{IC}$ (eq.S7)

$\Phi_{RISC} = \Phi_{TADF}/\Phi_{ISC}$ (eq.S8)

$k_{RISC} = (k_p k_{TADF} \Phi_{TADF})/(k_{ISC} \Phi_p)$ (eq.S9)

$k_p = 1/\tau_p$; $k_{TADF} = 1/\tau_{TADF}$ (eq.S10)

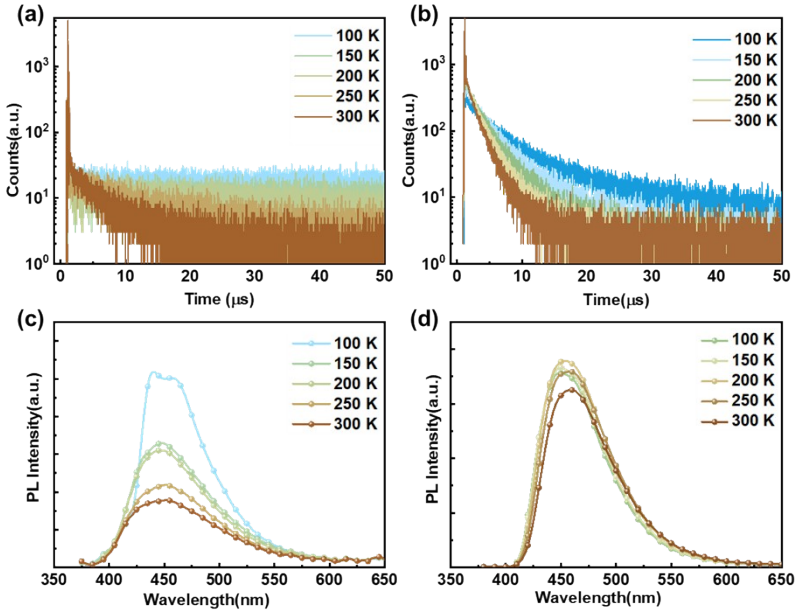

Fig. S1 Temperature-dependent time-resolved fluorescence spectra of compounds (a) **HO-DPS-DMAC** and (b) **F-DPS-DMAC**. The curves of PL intensity and peak position with increased temperature of compounds (c) **HO-DPS-DMAC** and (d) **F-DPS-DMAC**.

4. Single crystal data

Table S1. Crystal data and structure refinement for **HO-DPS-DMAC** (CCDC Number 2163495) and **F-DPS-DMAC** (CCDC Number 2472413)

Compound	**HO-DPS-DMAC**	**F-DPS-DMAC**
Empirical formula	$C_{27}H_{23}NO_3S$	$C_{27}H_{22}FNO_2S$
Formula weight	441.52	443.51
Temperature/K	173.00(10)	291.82(12)
Crystal system	monoclinic	monoclinic
Space group	$P2_1/n$	$P2_1/n$
a/Å	8.1193(3)	8.17384(17)
b/Å	17.2395(7)	17.3356(4)
c/Å	15.7214(5)	15.9288(4)
α/°	90	90
β/°	102.828(3)	103.372(2)
γ/°	90	90
Volume/Å^3	2145.65(14)	2195.89(10)
Z	4	4
ρ_{calc}g/cm^3	1.367	1.342
μ/mm^{-1}	0.182	1.583
F(000)	928.0	928.0
Crystal size/mm^3	0.21 × 0.15 × 0.14	0.22 × 0.17 × 0.15

Radiation	MoKα (λ = 0.71073)	CuKα (λ = 1.54184)
2Θ range for data collection/°	6.942 to 52.044	7.652 to 133.196
Index ranges	-10 ≤ h ≤ 10, -21 ≤ k ≤ 17, -19 ≤ l ≤ 18	-9 ≤ h ≤ 9, -17 ≤ k ≤ 20, -17 ≤ l ≤ 18
Reflections collected	7484	7812
Independent reflections	4211 [R_{int} = 0.0255, R_{sigma} = 0.0441]	3770 [R_{int} = 0.0292, R_{sigma} = 0.0324]
Data/restraints/parameters	4211/0/292	3770/84/354
Goodness-of-fit on F^2	1.092	1.036
Final R indexes [I>=2σ (I)]	R_1 = 0.0431, wR_2 = 0.1027	R_1 = 0.0500, wR_2 = 0.1426
Final R indexes [all data]	R_1 = 0.0537, wR_2 = 0.1129	R_1 = 0.0569, wR_2 = 0.1515
Largest diff. peak/hole / e $Å^{-3}$	0.33/-0.42	0.25/-0.27

Table S2. Some key packing parameters of the single crystals of **HO-DPS-DMAC** and **F-DPS-DMAC**

Compound	Number of H-bonds per molecule	Average distance of H-bond (Å)	Average distance of C-H···π intermolecular interactions (Å)	Average distance of C-H···O intermolecular interactions (Å)	Packing coefficient
HO-DPS-DMAC	1	2.740 (O-H···O)	2.867	2.591	69.63%
F-DPS-DMAC	1	2.249 (C-H···F)	3.040	2.500	69.44%

5. Thermal stability, electrochemical and EL properties of the compounds

The electrochemical characteristics of **HO-DPS-DMAC** and **F-DPS-DMAC** were measured by cyclic voltammetry using ferrocene as the reference material (Fig. S6).

$$E_{HOMO} = -4.8 - \left(E_c^{ox} - E_f^{ox}\right) \quad \text{(eq.S11)}$$

$$E_{LUMO} = E_{HOMO} + E_g \quad \text{(eq.S12)}$$

$$E_g = 1240/\lambda_{onset} \quad \text{(eq.S13)}$$

HO-DPS-DMAC and **F-DPS-DMAC** showed semi-reversible oxidation peaks. According to equation S11 to S13, the HOMO energy levels were calculated to be -5.43 eV and -5.51 eV, and the LUMO energy levels were calculated to be -2.04 eV and -2.55 eV.

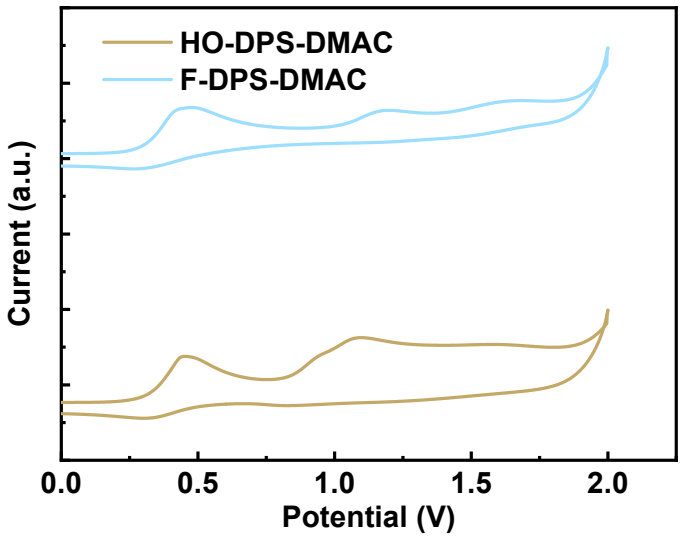

Fig. S2 Cyclic voltammogram curves of **HO-DPS-DMAC** and **F-DPS-DMAC** measured in toluene solution

HO-DPS-DMAC and **F-DPS-DMAC** exhibited excellent thermal stability with a decomposition temperature (T_d, corresponding to a 5% weight loss) at 330 °C and 313 °C (Figure S5), which was beneficial to the preparation and stability of OLED devices.

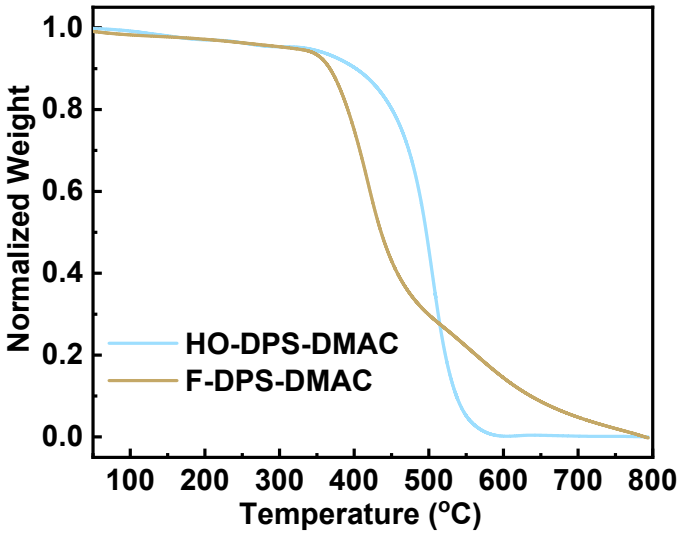

Fig. S3 TGA curves of **HO-DPS-DMAC** and **F-DPS-DMAC** in nitrogen atmosphere with a heating rate of 10 °C min^{-1}.

Table S3. Summarizes the performance of OLED devices based on **HO-DPS-DMAC** and **F-DPS-DMAC**

EML	V_{on}	λ_{EL} (nm)	L (cd m^{-2})	CE_{max} (cd A^{-1})	PE_{max} (lm W^{-1})	EQE_{max} (%)	CIE (x, y)
HO-DPS-DMAC	3.6	466	39.23	5.79	5.18	3.42	(0.19,0.30)
F-DPS-DMAC	6.6	481	147	4.95	1.84	2.56	(0.20,0.31)

6. NMR spectra

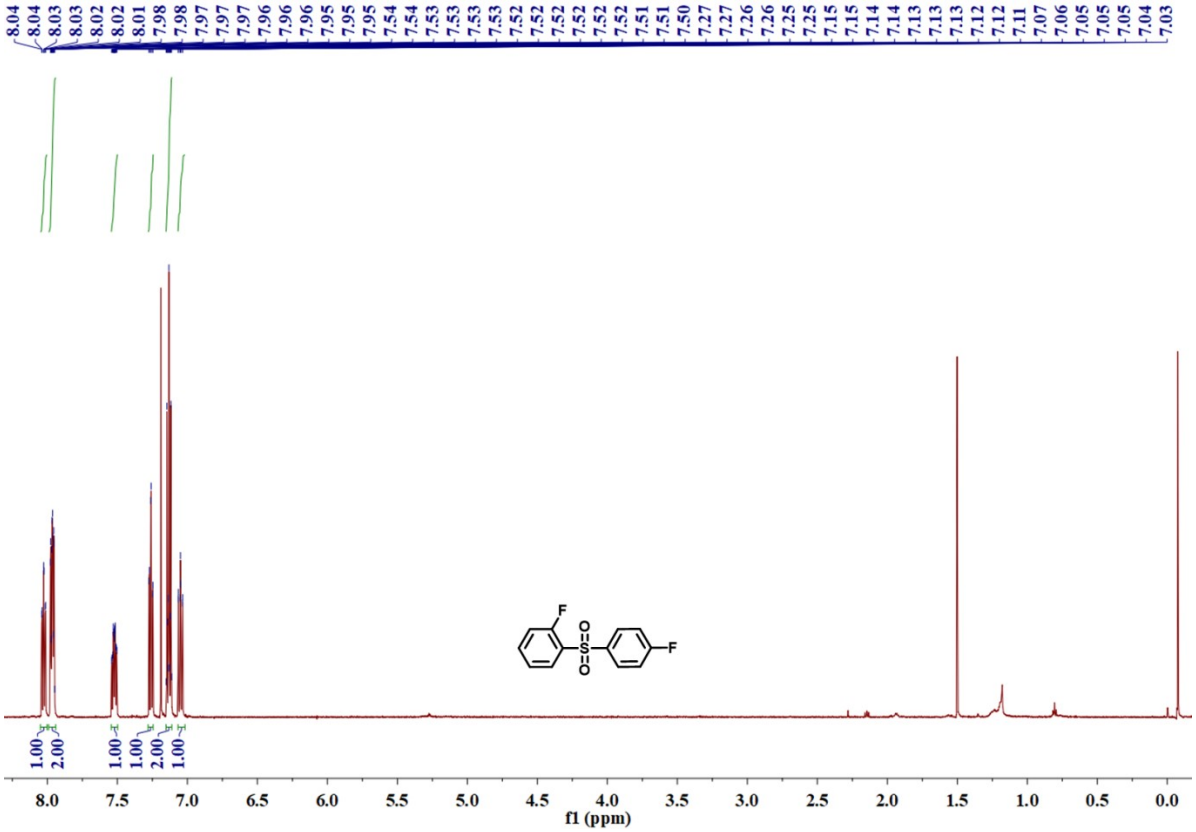

Fig. S4 ^{1}H NMR spectrum of **2, 4'-DF-DPS**

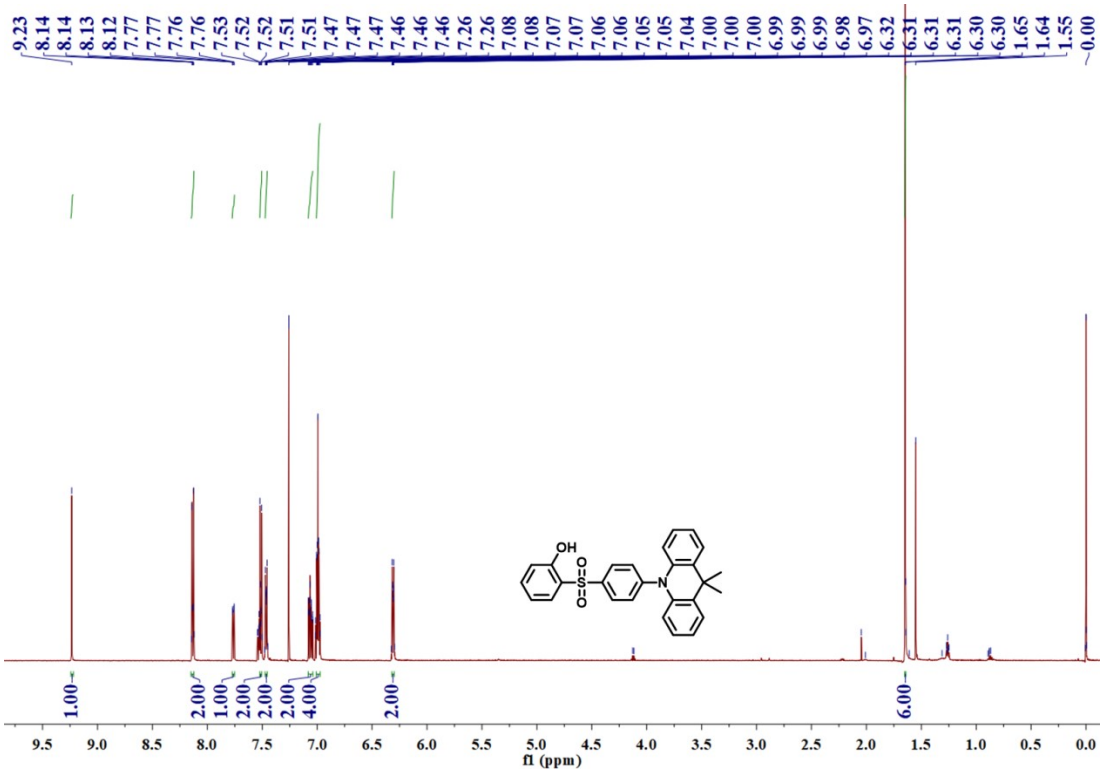

Fig. S5 ^{1}H NMR spectrum of **HO-DPS-DMAC**

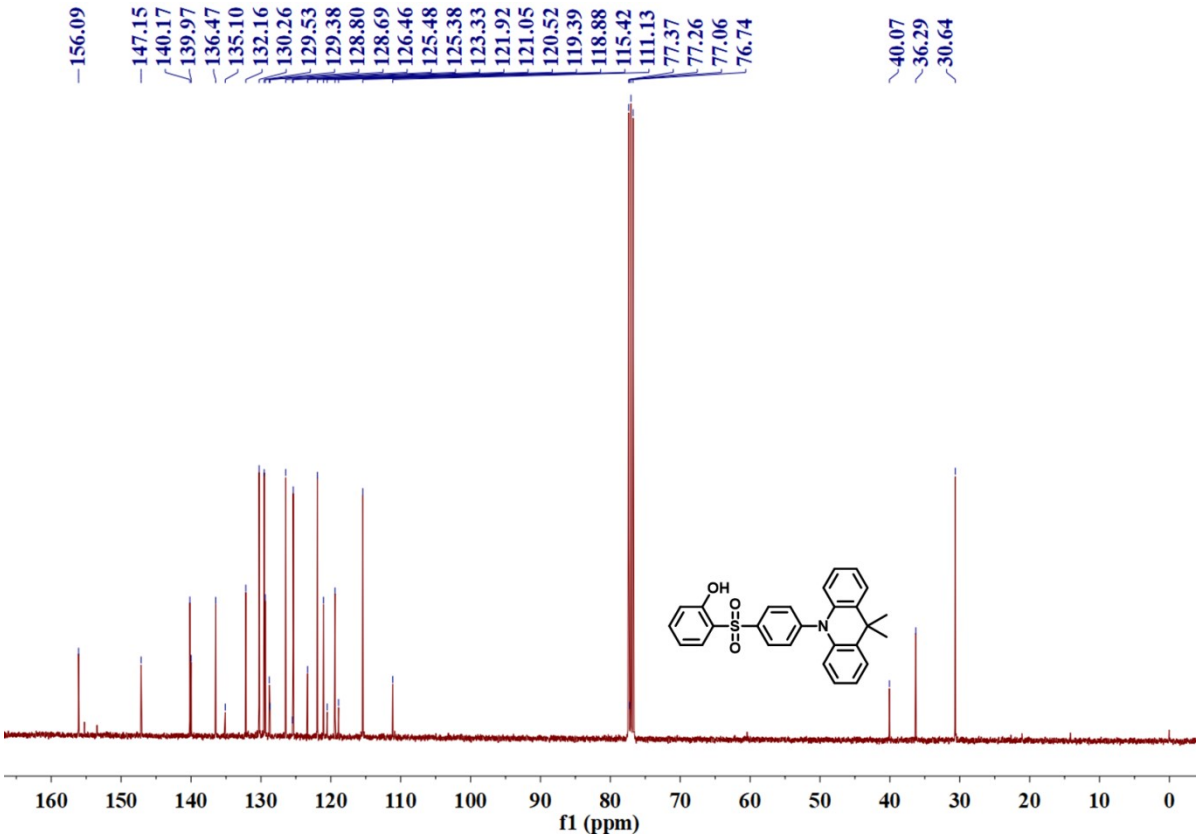

Fig. S6 ^{13}C NMR spectrum of **HO-DPS-DMAC**

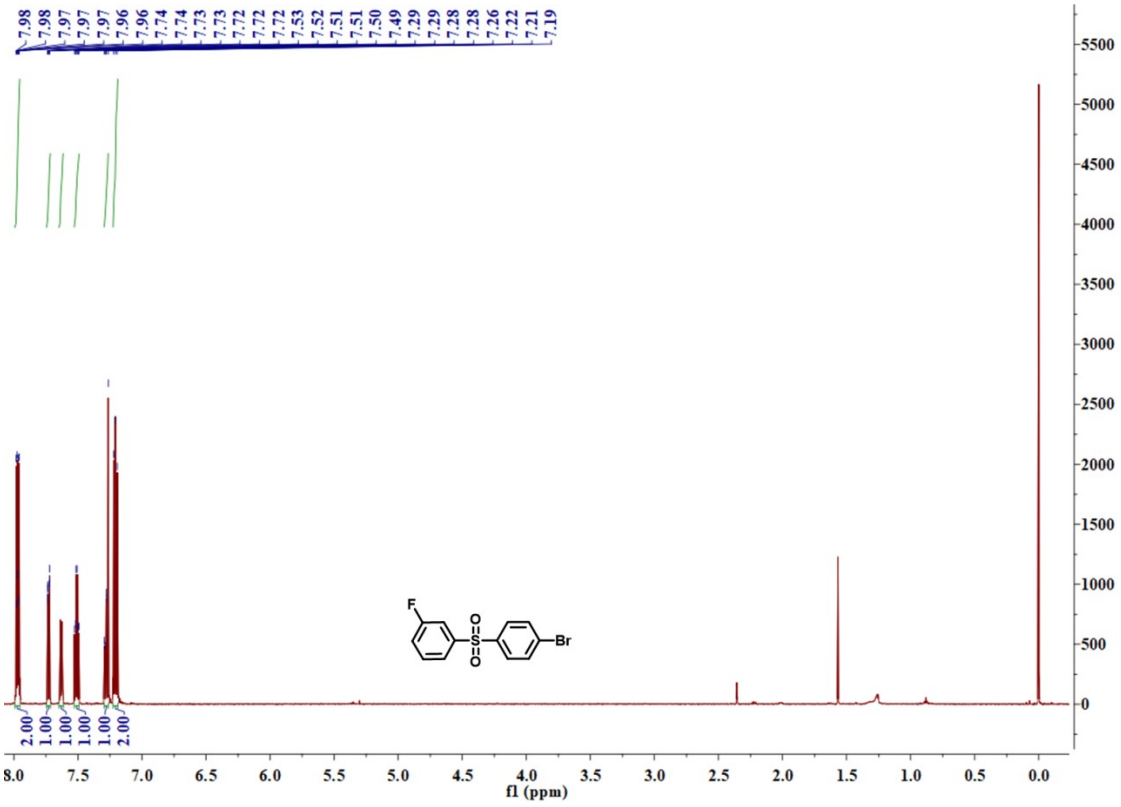

Fig. S7 ^{1}H NMR spectrum of **3-F-4'-Br-DPS**

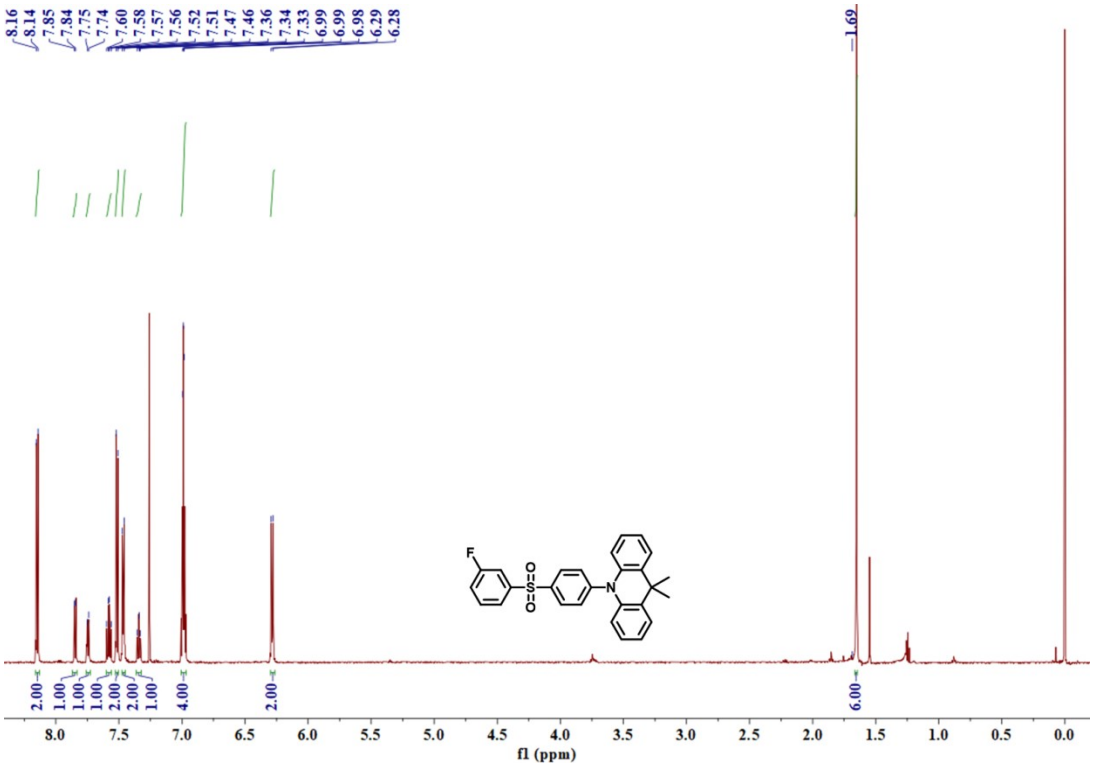

Fig. S8 ^{1}H NMR spectrum of **F-DPS-DMAC**

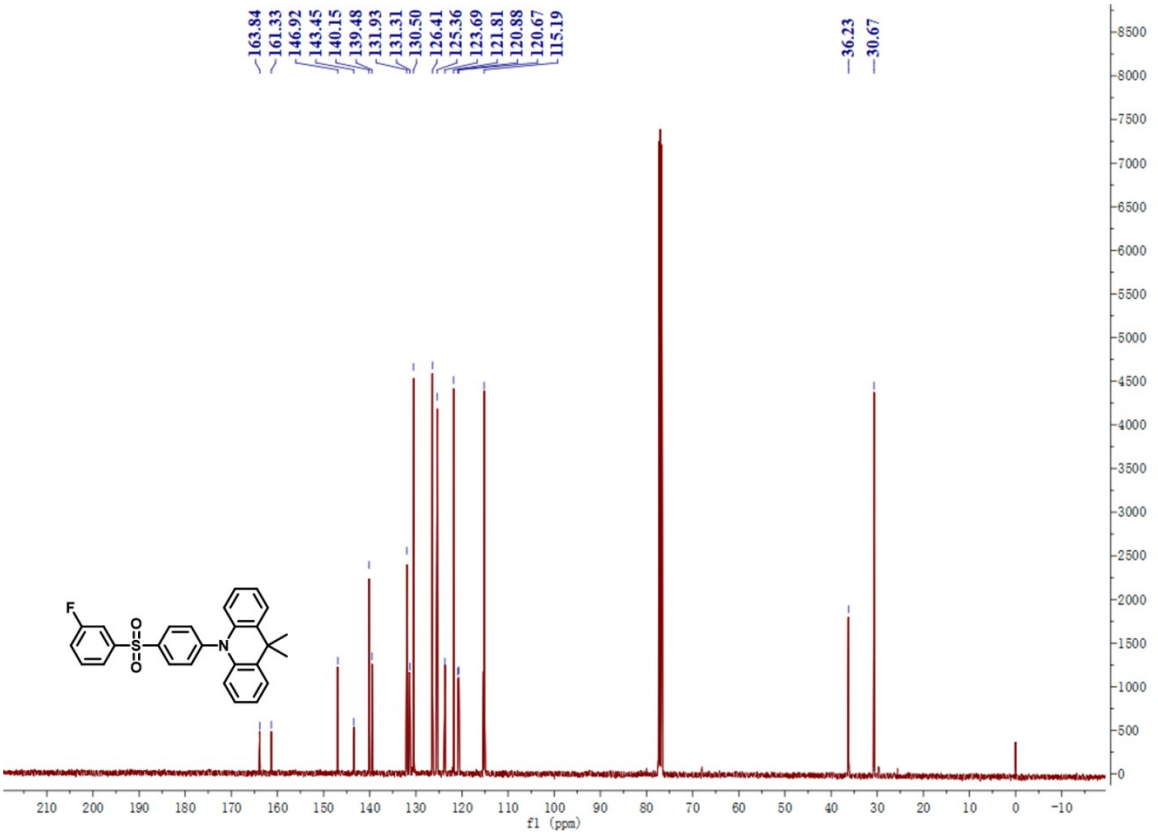

Fig. S9 ^{13}C NMR spectrum of **F-DPS-DMAC**

7. References

[S1] H. Uoyama, K. Goushi, K. Shizu, H. Nomura, C. Adachi, Highly efficient organic light-emitting diodes from delayed fluorescence, Nature 492(7428) (2012) 234-238. https://doi.org/10.1038/nature11687.

[S2] J. Xu, X. Zhu, J. Guo, J. Fan, J. Zeng, S. Chen, Z. Zhao, B. Z. Tang, Aggregation-Induced Delayed Fluorescence Luminogens with Accelerated Reverse Intersystem Crossing for High-Performance OLEDs, ACS Materials Letters 1(6) (2019) 613-619. https://doi.org/10.1021/acsmaterialslett.9b00369.

[S3] Q. Zhang, H. Kuwabara, W.J. Potscavage, Jr., S. Huang, Y. Hatae, T. Shibata, C. Adachi, Anthraquinone-based intramolecular charge-transfer compounds: computational molecular design, thermally activated delayed fluorescence, and highly efficient red electroluminescence, J Am Chem Soc 136(52) (2014) 18070-18081. https://doi.org/10.1021/ja510144h.